IOSR Journal of Engineering (IOSRJEN) **www.iosrjen.org**
ISSN (e): 2250-3021, ISSN (p): 2278-8719
Vol. 13, Issue 5, May 2023, ||Series -I|| PP 33-47

Numerical analysis of Magnetohydrodynamic micropolar Jeffrey fluid flow over linearly stretching sheet in porous medium with heat generation

Pravendra Kumar[1], Seema Goyal[2], Bhupander Singh[3], Kapil Kumar[4]
1-Research Scholar, Department of Mathematics, Meerut College, Meerut
2-Professor, Department of Mathematics, Meerut College, Meerut
3--Professor, Department of Mathematics, Meerut College, Meerut
4- Research Scholar, Department of Mathematics, Meerut College, Meerut

Abstract: A numerical approach to micropolar Jeffrey fluid flow over linearly stretching sheet is applied. The medium is taken porous in which sheet is stretching linearly. The governing equations of the problem are converted into similarity variables using suitable similarity transformation. The equations thus obtained are solved numerically by in built technique bvp4c in MATLAB. The influences of various pertinent parameters like micro-coupling parameter, Deborah number, Magnetic field parameter, Spin gradient viscosity parameter, Micro-inertia density parameter, Heat generation parameter, Lewis number, Prandtl number and Porosity parameter are depicted graphically.

Keywords Micropolar fluid, Heat generation, Jeffrey fluid, Magnetohydrodynamic, Porous medium, heat generation.

I. Introduction

Eringen [1] developed the idea of micropolar fluids, which contain microscopic components that connect the macroscopic velocity field and the rotating motion of the particles. Hard particles suspended in a fluid solution make up these fluids. The formation of colloidal fluids, liquid crystals, biological structures, etc. may all be explained using this idea. A controlled cooling system is necessary since cooling speed is crucial for product manufacturing. Since thermal radiation is a well-understood phenomenon, it has become quite simple to deal with the extreme heat produced by numerous industrial activities, including nuclear reactors, spacecraft, etc. A heated surface emits electromagnetic radiation in all directions, which travels at the speed of light directly to its point of absorption in the process known as thermal radiation. A surface's total radiant heat energy is proportional to the fourth power of its absolute temperature, creating a term for the heat gradient in the energy equation. The flow behavior of non-Newtonian fluids cannot be described by the traditional Navier-Stokes equations. As a result, the literature suggests various non-Newtonian model types. The non-Newtonian fluid has drawn the attention of researchers over the last few years, as is evident from its use in business and the creative world. Non-Newtonian liquids frequently behave differently from Newtonian liquids, especially in a few designing applications. One of the rate type materials is a subclass of non-Newtonian liquids called Jeffrey fluid. It demonstrates the fluid's linear viscoelastic action, which has numerous uses in the polymer industry. Jeffrey fluid can have several forms, one of which is diluted polymer solution. Most fluid models use the Jeffrey fluid, a less difficult direct model that uses time derivative rather than convected derivative. The characteristics of retardation and relaxation times can be represented using this liquid model. A few of these fluids are discussed in (Hayat and Mustafa [2], Hayat and Obaidat [3], Nadeem and Fang [4], Turkyilmazoglu and Pop [5], and Qasim [6]). The Jeffrey fluid was also utilized by Sharma et al. [7] to simulate the flow of blood through small arteries. An examination into the effects of a magnetic field on the flow of the Jeffrey fluid in small tubes in a porous media was conducted by Nallapu and Radhakrishnamacharya [8]. Heat transfer in MHD micropolar Jeffery fluid flow over a stretching sheet in porous medium in the presence of thermal radiation investigated and solved numerically by vandna et al.[9]. Other studies on the Jeffrey model have been conducted by Ellahi et al. [10], Khan et al. [11], and Vaidya et al. [12].

Das et al. [13] investigation radiative flow of MHD Jeffrey fluid past a stretching sheet with surface slip and melting heat transfer .Vandna et al. [14] studied the MHD micropolar fluid flow over a permeable channel and thermal radiation is also taken into account for the problem. They obtained an analytic solution of the problem by perturbation method (HPM).MHD heat transfer fluid flow over a stretching cylinder thorough a porous medium in the presence of heat generation/absorption effect studied by Dhermendar et al.[15]. They show that when rise in the curvature parameter and porosity parameter, the temperature gradient also increased in the boundary layer area around the cylinder. Mahabaleshwar et al. [16] investigated and solved numerically a MHD fluid flow heat transfer over a stretching/shrinking sheet in the presence of heat source/sink and thermal

radiation effects by using CNTs. The upper branch solutions of the magnetic field profile are analytically stable compared to the lower branch solutions. The relation between nonlinear mixed convection and thermal radiation in the case of Newtonian fluid flow over non linear stretching sheet investigated and solved numerically Panday et al. [17]. They demonstrate that when linear convection parameter increases, the flow velocity increases near the sheet and decreases away from the sheet. Megahed et al. [18] examined the analysis of MHD flow near an unstable stretched sheet with varying fluid characteristics, thermal radiation, and heat flux. On MHD unsteady free convective rotating flow by Jeffrey fluid having ramping wall temperature, Krishna [19] investigated the ion slip and Hall effects. Khader et al. [20] found the numerical solution of MHD unsteady micropolar fluid flow caused by stretched/shirked surface with thermal radiation and heat source. The study of the motion of electrically conducting fluids in the presence of a magnetic field, or the interaction of a magnetic field and the fluid velocity of such fluids, is known as magnetohydrodynamics (MHD). Examples of such systems include dynamos and MHD pumps. Many studies employ the MHD flow with heat and mass transfer because of the primary effect of the magnetic field [21], [22], [23], [24]. The varied characteristics of MHD non-Newtonian fluid flow over a stretching surface were examined by Adegbie et al. [25] and Malik et al. [26]. It was determined that a changing thermal conductivity value increases fluid temperature. Study that is analytical and numerical electrically conductive fluid is now a significant component of many engineering scientific fields, including MHD generators and nuclear reactors, among others. Additionally, it has a wide range of important technological and industrial applications, including biometric pumps, smart lubrication systems, and device separation. In the domain of biological fluids, many researchers have considered MHD studies [27], [28]. The study of convective heat transfer in fluid-saturated porous media has drawn attention because of the wide range of industries it can be applied to, particularly geothermal energy recovery, food processing, fibre and granular insulation, packed bed reactor design, and dispersion of chemical contaminants in various chemical industry and environmental processes [29]. In a porous medium with a low pressure gradient, Ahmed et al. [30] studied the effects of radiation on MHD boundary layer convective heat transport. Through a porous media, Butt et al. [31] discovered heat production effects on MHD Jeffery fluid.

Mathematical formulation

A steady two-dimensional incompressible Jeffrey micropolar fluid flow in a porous medium over a stretching sheet coinciding with the plane y=0 is considered, and the flow is confined to the plane y > 0. The surface is assumed to stretch linearly with velocity$U_w = ax$, where a is stretching constant. Here, the co-ordinates (x, y) are such that the x-axis is chosen parallel to the vertical surface, and the y-axis is taken normal to it, and (u, v) are the velocity components of the flow, and N defines the internal speed of the micropolar particles. **g** defines the gravity. A uniform magnetic field of strength B_0 is applied normal to the sheet. (Fig.1.).

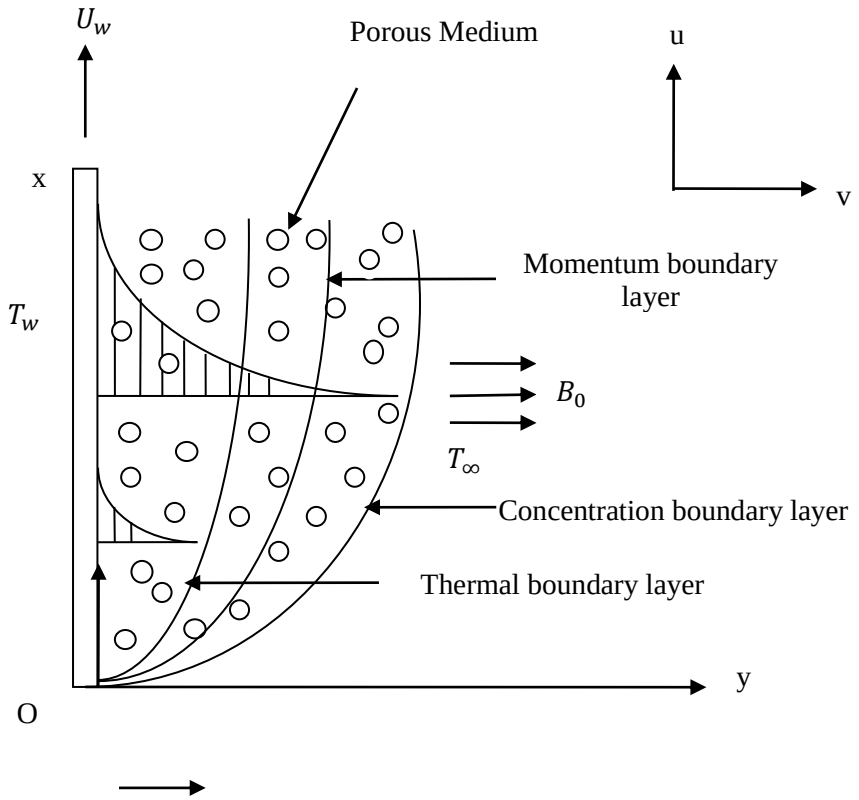

The governing equations with corresponding boundary conditions for the said problem are

$$\frac{\partial u}{\partial x}+\frac{\partial v}{\partial y}=0 \tag{1}$$

$$u\frac{\partial u}{\partial x}+v\frac{\partial u}{\partial y}=\frac{\left(\vartheta+\frac{K}{\rho}\right)}{(1+\lambda_2)}\left[\frac{\partial^2 u}{\partial y^2}+\lambda_1\left(u\frac{\partial^3 u}{\partial x\partial y^2}+v\frac{\partial^3 u}{\partial y^3}-\frac{\partial u}{\partial x}\frac{\partial^2 u}{\partial y^2}+\frac{\partial u}{\partial y}\frac{\partial^2 u}{\partial x\partial y}\right)\right]-\frac{\sigma B_0^2 u}{\rho}+\left(\frac{K}{\rho}\right)\frac{\partial N}{\partial y}-\frac{\mu u}{K^*\rho} \tag{2}$$

$$u\frac{\partial N}{\partial x}+v\frac{\partial N}{\partial y}=\frac{\gamma}{\rho_j}\frac{\partial^2 N}{\partial y^2}-\frac{\kappa}{\rho_j}\left(2N+\frac{\partial u}{\partial y}\right) \tag{3}$$

$$u\frac{\partial T}{\partial x}+v\frac{\partial T}{\partial y}=\propto\frac{\partial^2 T}{\partial y^2}+\frac{Q}{(\rho C_p)_f}(T-T_\infty) \tag{4}$$

$$u\frac{\partial C}{\partial x}+v\frac{\partial C}{\partial y}=D_B\frac{\partial^2 C}{\partial y^2} \tag{5}$$

Where u and v are the velocity components in the x and y directions, respectively λ_1 is the ratio of the relaxation and retardation time, λ_2 is the relaxation time, T is the fluid temperature, $\nu=\frac{\mu}{\rho}$ is the kinematic viscosity, μ is the coefficient of fluid viscosity, ρ is the fluid density, K^* is the permeability of the porous medium, κ is thermal conductivity of fluid, C_p is specific heat at constant pressure, D_B Brownian diffusion and α is thermal diffusivity.

The boundary conditions of the problem are defined as follows

$$u=U_w\,, v=0, T=T_w, N=0\ at\ y=0 \tag{6}$$

$$u\to 0, N\to 0, T\to T_\infty, \frac{\partial u}{\partial y}\to 0\ at\ y\to\infty \tag{7}$$

The sheet velocity and temperature are U_w and T_w , respectively, and are assumed to be

$$U_w=ax\,, T_w=T_\infty+bx\,, \text{b are positive constants} \tag{8}$$

Here by introducing the following Similarity variables, we have

$$\eta=y\sqrt{\frac{a}{\upsilon}}\,,\ \psi=\sqrt{a\upsilon}xf(\eta),\ \ N=a\sqrt{\frac{a}{\upsilon}}xg(\eta),\ \theta(\eta)=\frac{T-T_\infty}{T_w-T_\infty} \tag{9}$$

$$u=\frac{\partial\psi}{\partial y}\,,\qquad v=-\frac{\partial\psi}{\partial x}$$

Where $\psi=\psi(x,y)$ is the stream function are

Using Similarity Transformations (9), Equation (2), (3), (4) and (5) become

$$(1+A_1)f'''+(1+\lambda_2)\left[ff''-f'^2+A_1g'-\left(M+K_p\right)f'\right]+(1+A_1)\beta\left(f''^2-f^{iv}\right)=0 \tag{10}$$

$$\lambda_o g''+g'f-gf'-A_1B(2g+f'')=0 \tag{11}$$

$$f\theta'+\frac{\theta''}{P_r}+\Delta\theta=0 \tag{12}$$

$\phi'' + L_e P_r f \phi' = 0$ (13)

Where

$$A_1 = \frac{K}{\mu}, \quad \beta = a\lambda_1, \quad M = \frac{\sigma B_o^2}{a\rho}, \quad K_p = \frac{\upsilon}{a\mathrm{K}^*}, \quad \mu = \upsilon\rho, \quad \lambda_o = \frac{\gamma}{\mu j}, \quad B = \frac{\upsilon}{ja}, \quad P_r = \frac{\upsilon}{\alpha},$$

$$\Delta = \frac{Q}{a(\rho C_p)_f}, \quad L_e = \frac{\alpha_f}{D_B}$$

The non-dimensional parameters $A_1, \beta, M, \lambda_o, B, \Delta,$ and L_e represent micro-coupling parameter , Deborah number, magnetic field parameter, spin gradient viscosity parameter, micro-inertia density parameter, heat generation parameter and Lewis parameter, respectively, where as Pr and Kp represent Prandtl number and porosity parameter, respectively.

Boundary conditions defined by (6) and (7) are uniquely formed in similarity as follows

$f(0) = 0, f'(0) = 1, \theta(0) = 1, g(0) = 0 \; at \; \eta = 0$ (14)

$f'(\eta) \to 0, g(\eta) \to 0, \theta(\eta) \to 0, f'' \to 0 \; at \; \eta \to \infty$ (15)

Some of essential physical parameters, like skin coefficient and Nusselt's number, which are defined as.

$C_f = \frac{2T_w}{\rho U_w^2} \; and \; N_u = \frac{q_w}{T_w - T_\infty}\left(\frac{x}{K}\right)$.where $T_w = -\frac{\mu}{1+\lambda_2}\left[\left[\frac{\partial u}{\partial y} + \lambda_1\left(u\frac{\partial^2 u}{\partial x \partial y} + v\frac{\partial^2 u}{\partial y^2}\right)\right] + \frac{K}{\mu}(N)\right]$ at y=0 and

$q_w = -\kappa\left(\frac{\partial T}{\partial y}\right)$ at y=0

Therefore,

$\frac{1}{2}(1+\lambda_2)C_f\sqrt{R_e} = -[f''(0) + \beta f''(0)] = -f''(0)[1+\beta]$ (16)

$\frac{N_u}{\sqrt{R_e}} = -\theta'(0)$ (17)

Solution algorithm

To solve boundary value problems (10)-(13) with boundary conditions given by (14) and (15), we used built-in solver called bvp4c function in MATLAB software package. The algorithm is based on to reduce the nonlinear ordinary differential equations (10)-(13) with boundary conditions (14) and (15) into the system of first order nonlinear differential equations as follows.

$f = y_1, f' = y_2, f'' = y_3, f''' = y_4, g = y_5, g' = y_6, \theta = y_7, \theta' = y_8, \phi = y_9, \phi' = y_{10}$ (18)

Using (16), Equation (8)-(10) reduce to first order nonlinear ordinary differential equations

$y_1' = y_2$ (19)

$y_2' = y_3$ (20)

$y_3' = y_4$ (21)

$y_4' = y_3^2 + \frac{y_4}{\beta} + \frac{(1+\lambda_2)}{(1+A_1)\beta}\left[y_1 y_3 - y_2^2 + A_1 y_6 - (M + K_p)y_2\right]$ (22)

$y_5' = y_6$ (23)

$y_6' = \frac{1}{\lambda_0}[y_2 y_5 - y_1 y_6 + A_1\beta(2y_5 + y_3)]$ (24)

$y_7' = y_8$ (25)

$y_8' = -P_r[y_1 y_8 + \Delta y_7]$ (26)

$y_9' = y_{10}$ (27)

$y_{10}' = -L_e P_r y_1 y_{10}$ (28)

Graphical results and discussion

The objective of the present paper is to study the steady MHD micropolar Jeffery fluid flow over linearly stretching sheet in porous medium with heat generation. The transformed Equations (10), (11), (12) and (13) along with the boundary conditions (14) and (15) were solved numerically by the bvp4c (boundary value problem fourth order Runge–Kutta collocation method) routine in MATLAB software and the results thus obtained were developed into graphs in which the behaviour of non-dimensional parameters like micro-coupling parameter, Deborah number, magnetic field parameter, spin gradient viscosity parameter, micro-inertia density parameter, heat generation parameter and Lewis parameter etc. The impact of pertinent parameters on the simulate velocity, temperature, concentration, skin friction coefficient, and micro-rotation is been discussed in this section. To illustrate the computed results, some figures are plotted and explained.

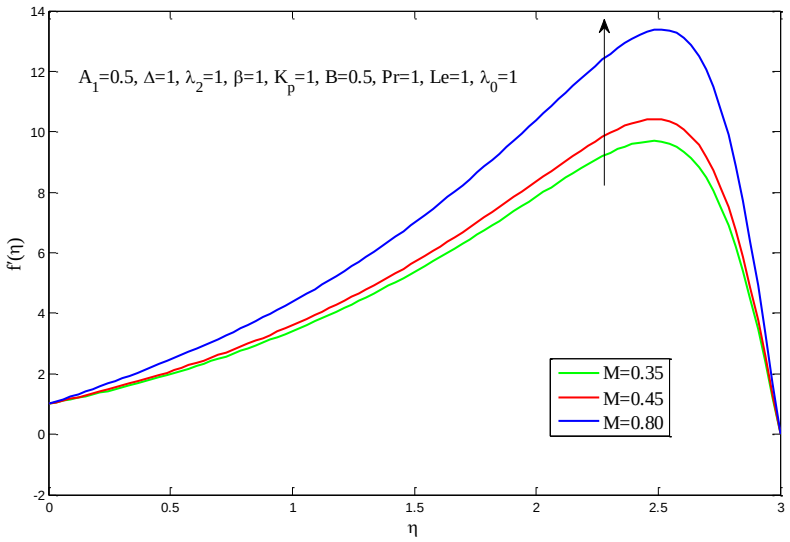

Fig. 2 Effect of magnetic field parameter on simulated velocity

Figure 2 shows the effect of magnetic field on fluid velocity as M is increasing fluid velocity gradually increases from surface of the sheet to outwards and tumbling down with other parameters $A_1 = 0.5, \Delta = 1, \lambda_2 = 1, \beta = 1, Kp = 1, B = 0.5, Pr = 1, Le = 1, \lambda_0 = 1$

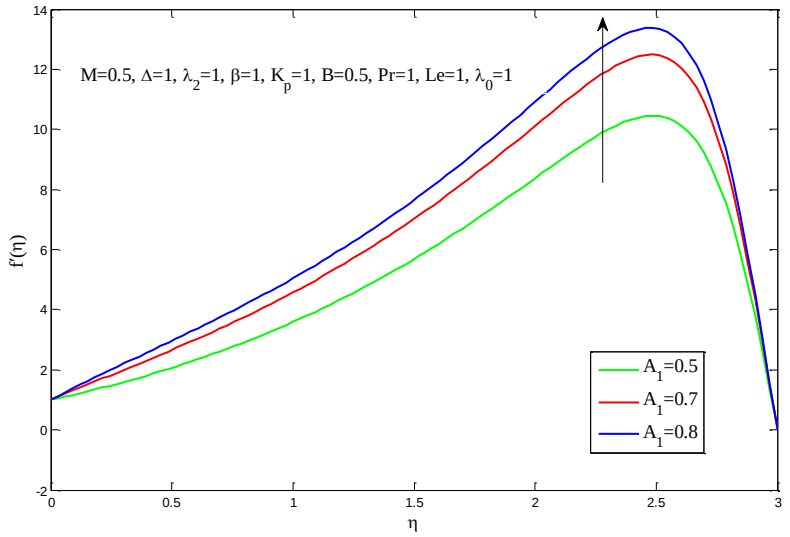

Fig. 3 Effect of coupling parameter on Simulated velocity

Figure 3 shows the effect on the rise of coupling parameter directly affects the value of simulated velocity , as the coupling parameter is directly proportional to the simulated velocity ; similarly if we increase the value of coupling parameter, the value of simulated velocity increases above the surface and then falls below. $M = 0.5, \Delta = 1, \lambda_2 = 1, \beta = 1, Kp = 1, B = 0.5, Pr = 1, Le = 1, \lambda_0 = 1$

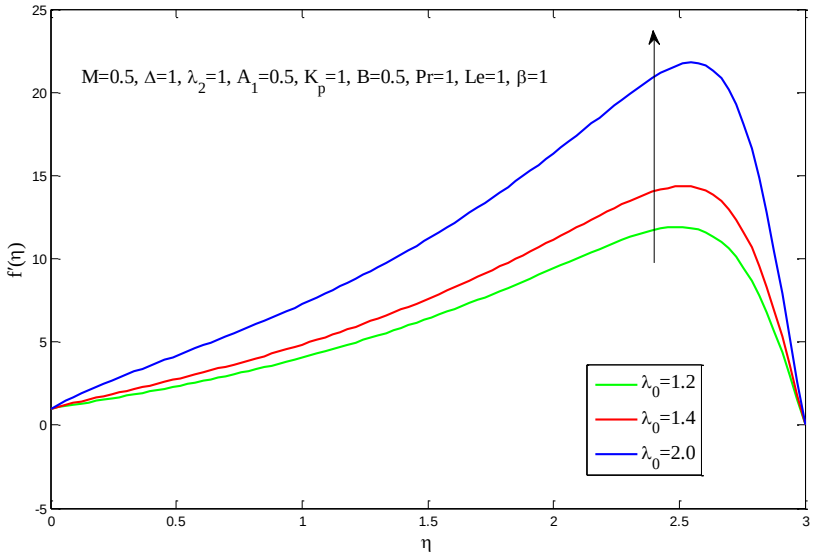

Fig. 4 Effect of spin gradient viscosity parameter on Simulated velocity

Figure 4 Display the effect of the spin gradient viscosity on the value of the simulated velocity it may also depicts the raise of the simulated velocity on the increase spin gradient viscosity parameter. $A_1 = 0.5, \Delta = 1, \lambda_2 = 1, \beta = 1, Kp = 1, B = 0.5, Pr = 1, Le = 1, M = 0.5$

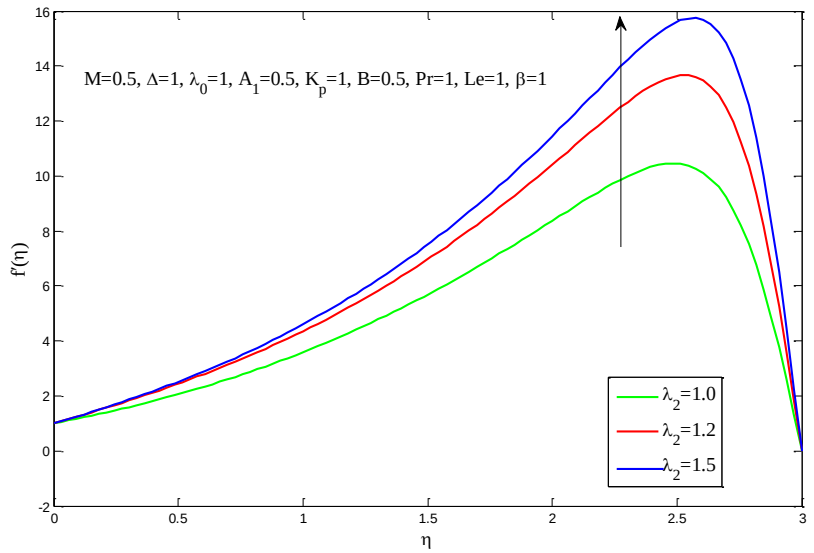

Fig. 5 Effect of Jeffrey fluid parameter on Simulated velocity

Figure 5 denotes the effect of Jeffrey Fluid on the simulated velocity, according to the above graph we can say that if we increase the value of Jeffrey Fluid parameter then the simulated velocity will also increased $A_1 = 0.5, \Delta = 1, \lambda_0 = 1, \beta = 1, Kp = 1, B = 0.5, Pr = 1, Le = 1, M = 0.5$

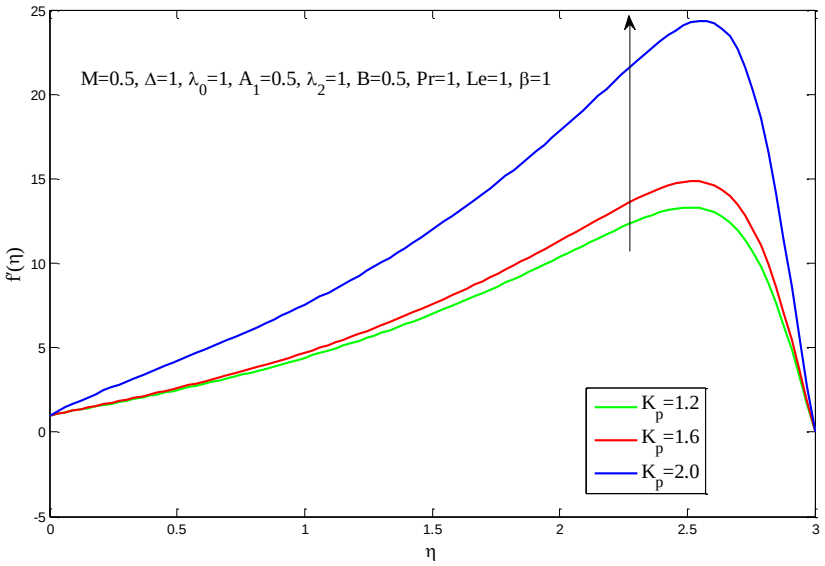

Fig. 6 Effect of porosity parameter on Simulated velocity

Figure 6 involve the action on increasing the value of porosity parameter on the simulated velocity, this shows that if we increase the porosity parameter the velocity will simultaneously increased $A_1 = 0.5, \Delta = 1, \lambda_2 = 1, \beta = 1, \lambda_0 = 1, B = 0.5, Pr = 1, Le = 1, M = 0.5$

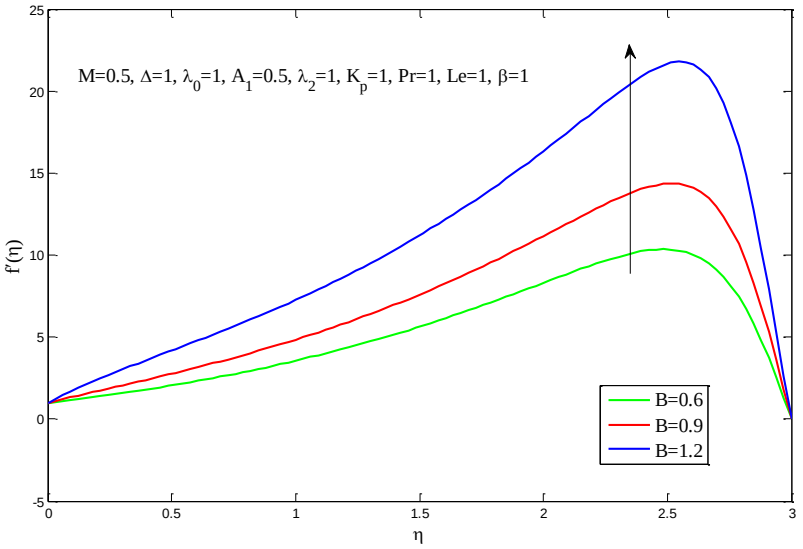

Fig. 7 Effect of micro-inertia density parameter on Simulated velocity

Figure 7 displays the effect of micro-inertia density parameter on simulated velocity; this explains that if we increase the micro inertia density parameter the simulated velocity will increase $A_1 = 0.5, \Delta = 1, \lambda_2 = 1, \beta = 1, \lambda_0 = 1, Kp = 1, Pr = 1, Le = 1, M = 0.5$

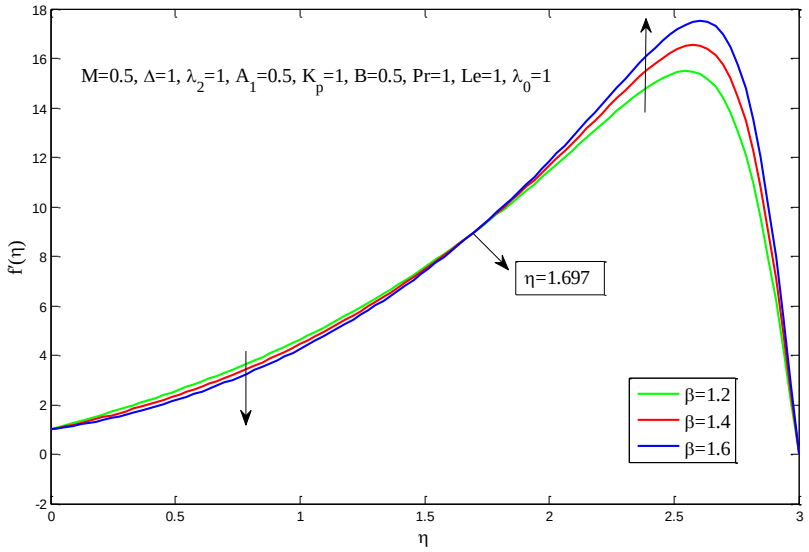

Fig. 8 Effect of Deborah number on Simulated velocity

Figure 8 portrays the effect of the Deborah number on simulated velocity. Velocity profile decreases as Deborah number increases, but after reaching η=1.697, the velocity increases. In the presence of the Deborah number, the fluid oscillates irregularly in the middle of the channel.

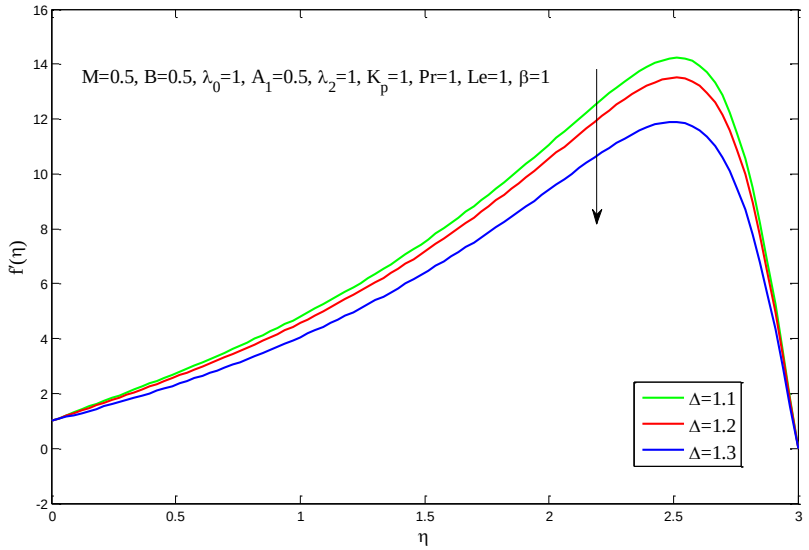

Fig. 9 Effect of heat generation parameter on Simulated velocity

Figure 9 denotes the significance of heat generation parameter on simulated velocity, by this graph we can clearly observe that by increasing the heat generation parameter, the simulated velocity will decrease $A_1 = 0.5, Kp = 1, \lambda_2 = 1, \beta = 1, \lambda_0 = 1, B = 0.5, Pr = 1, Le = 1, M = 0.5$

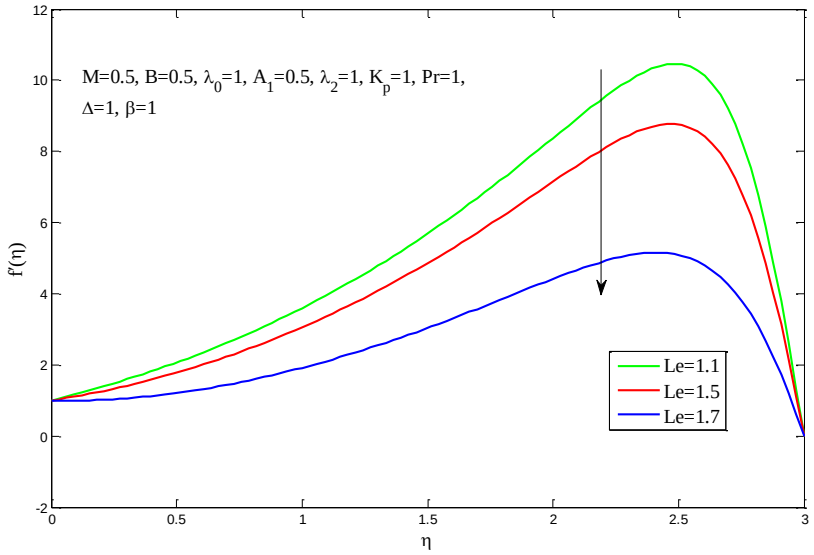

Fig. 10 Effect of Lewis parameter on Simulated velocity

Figure 10 describes the effect of Lewis parameter on simulated velocity, by this graph we can observe that Lewis parameter is inversely proportional to simulated velocity, hence by increasing the Lewis parameter the velocity decreases $A_1 = 0.5, \Delta = 1, \lambda_2 = 1, \beta = 1, \lambda_0 = 1, B = 0.5, Pr = 1, Kp = 1, M = 0.5$

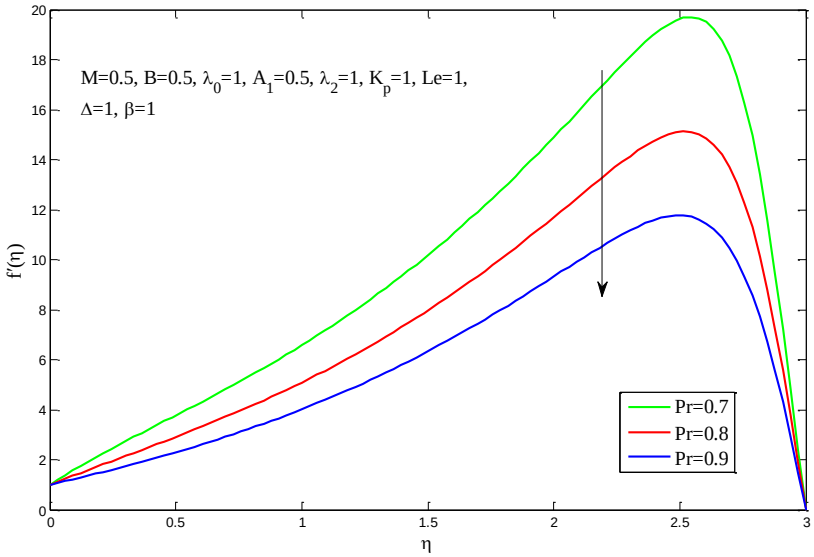

Fig. 11 Effect of Prandtl number on Simulated velocity

Figure 11 shows the effect of Prandtl number on the simulated velocity, this graph displays that on increasing the value of Prandtl number the simulated velocity decreases $A_1 = 0.5, \Delta = 1, \lambda_2 = 1, \beta = 1, \lambda_0 = 1, B = 0.5, Kp = 1, Le = 1, M = 0.5$

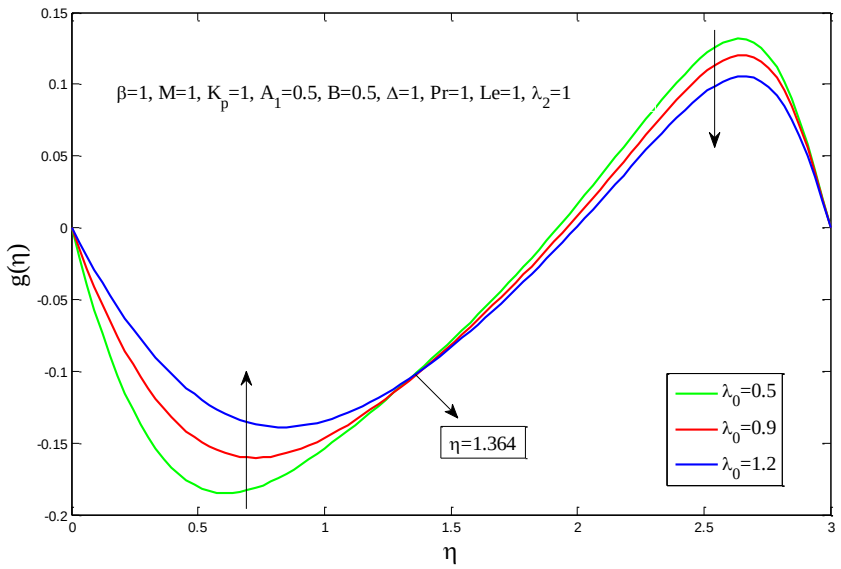

Fig. 12 Effect of spin gradient viscosity parameter on Micro-rotation

Figure 12 exhibits influence of spin gradient viscosity parameter on micro-rotation, this graph depicts that the value of micro-rotation will increase until it reaches $\eta = 1.364$, after this number the value of micro-rotation will decrease $A_1 = 0.5, \Delta = 1, \lambda_2 = 1, \beta = 1, Pr = 1, B = 0.5, Kp = 1, Le = 1, M = 0.5$

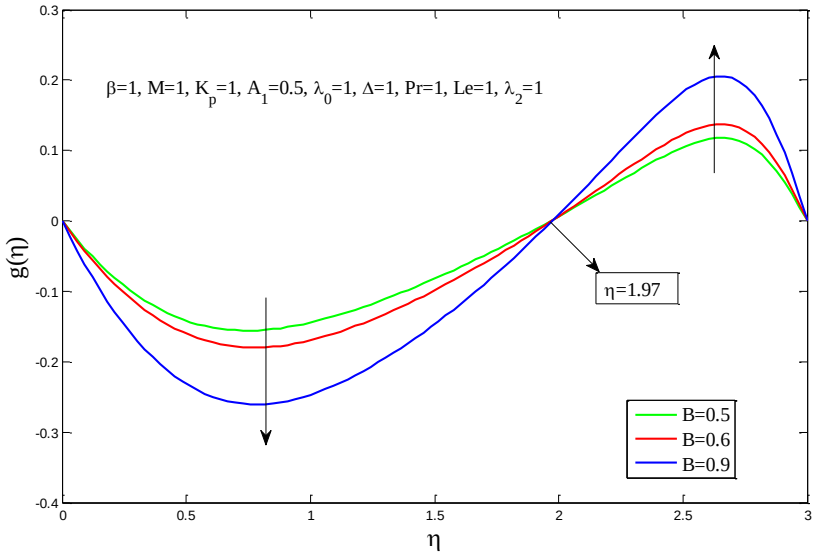

Fig. 13 Effect of micro-inertia density parameter on Micro-rotation

Figure 13 explains the effect of micro-inertia density parameter on micro-rotation, this results that the value micro-rotation will decrease until it reaches the $\eta = 1.97$, then it will start to increase certainly $A_1 = 0.5, \Delta = 1, \lambda_2 = 1, \beta = 1, Pr = 1, \lambda_1 = 1, Kp = 1, Le = 1, M = 0.5$

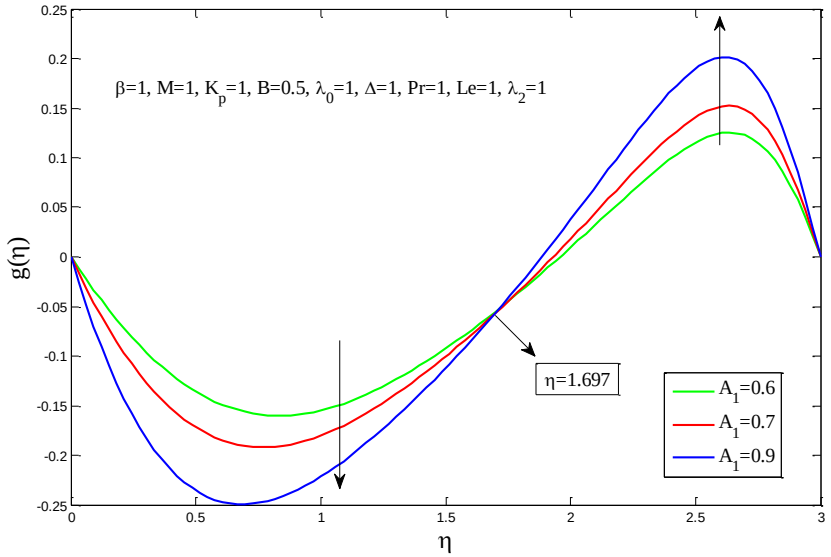

Fig. 14 Effect of coupling parameter on Micro-rotation

Figure 14 enrolls the effect of coupling parameter on micro rotation, this explains that the micro-rotation will decrease until the coupling parameter reaches $\eta = 1.697$, after this the micro-rotation increases$B = 0.5, \Delta = 1, \lambda_2 = 1, \beta = 1, Pr = 1, \lambda_1 = 1, Kp = 1, Le = 1, M = 0.5$

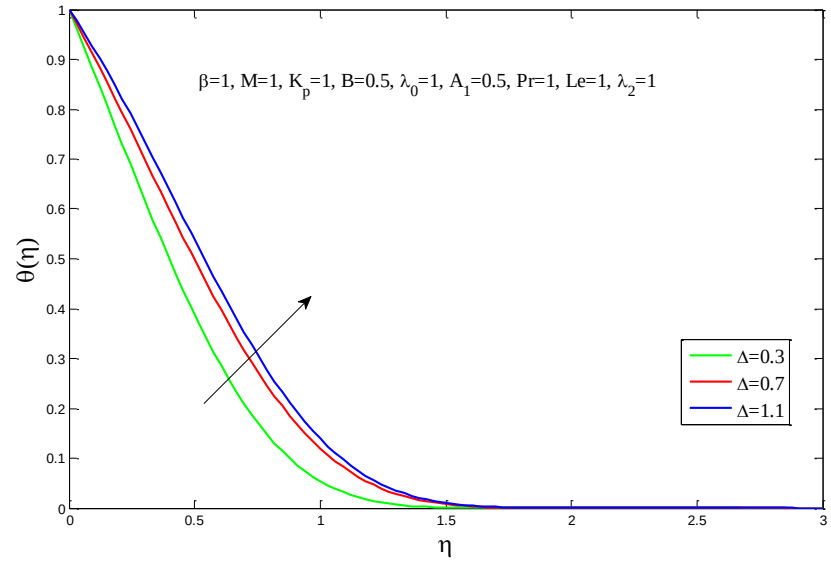

Fig. 15 Effect of Δ on Temperature

Figure 15 portrays the effect of heat generation parameter on Temperature, the following graph displays that the temperature will simultaneously increase, with the increase in the heat generation parameter $B = 0.5, A_1 = 0.5, \lambda_2 = 1, \beta = 1, Pr = 1, \lambda_1 = 1, Kp = 1, Le = 1, M = 0.5$

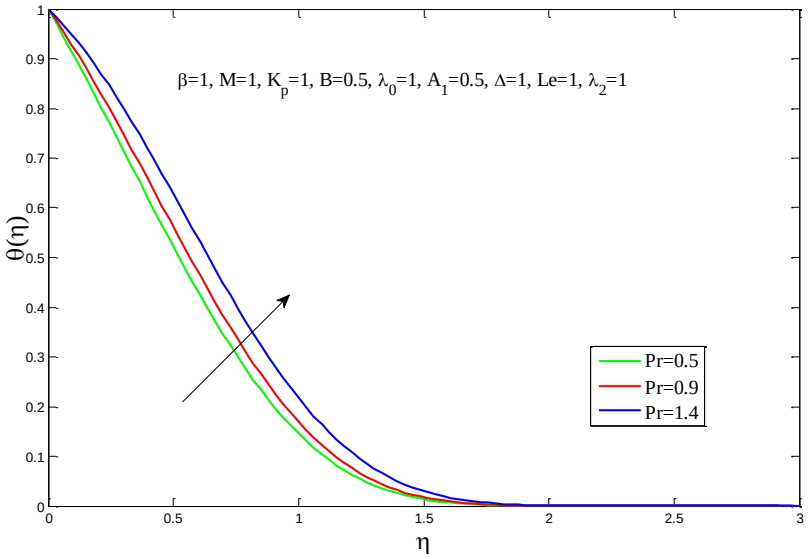

Fig. 16 Effect of Pr on Temperature

Figure 16 depicts the effect of Prandtl number on Temperature; this graph shows that the Temperature will increase with the increase in the value of Prandtl number $B = 0.5, A_1 = 0.5, \lambda_2 = 1, \beta = 1, \Delta = 1, \lambda_1 = 1, Kp = 1, Le = 1, M = 0.5$

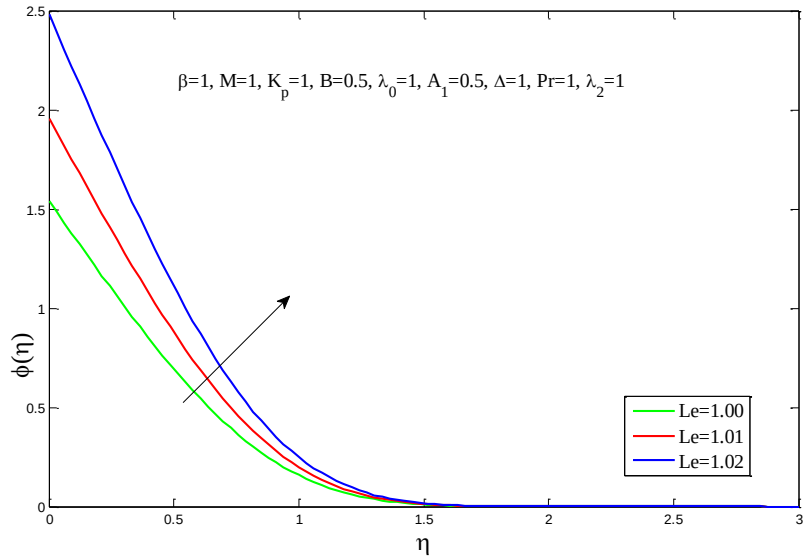

Fig. 17 Effect of Le on concentration profile

Figure 17 shows the effect of Lewis parameter on the concentration profile, according to this graph while the increase in the value of the Lewis parameter the value of concentration profile will also increase $B = 0.5, A_1 = 0.5, \lambda_2 = 1, \beta = 1, \Delta = 1, \lambda_0 = 1, Kp = 1, Pr = 1, M = 0.5$

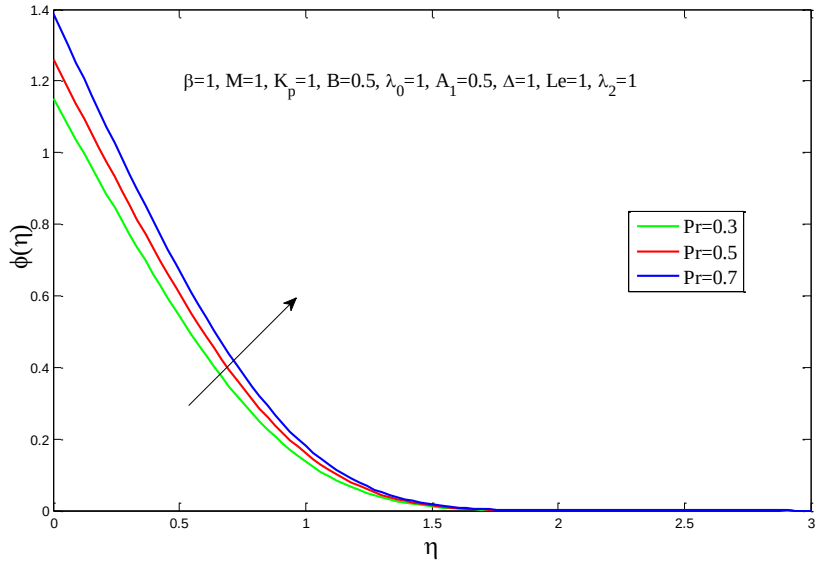

Fig. 18 Effect of Pr on concentration profile

Figure 18 displays the effect of Prandtl number on the concentration profile, the graph depicts that the concentration profile increases, with the increase in the Prandtl number $B = 0.5, A_1 = 0.5, \lambda_2 = 1, \beta = 1, \Delta = 1, \lambda_0 = 1, Kp = 1, Le = 1, M = 0.5$

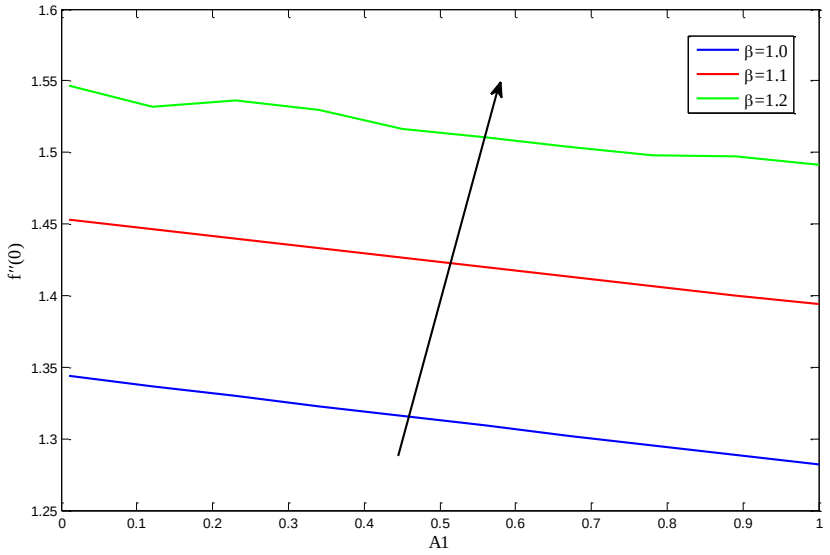

Fig. 19 impact of β and A_1 on skin friction coefficient

Figure 19 portrays the impact of β on the skin friction coefficient; the above graph shows that on increasing the value of β the value of skin friction coefficient increases simultaneously

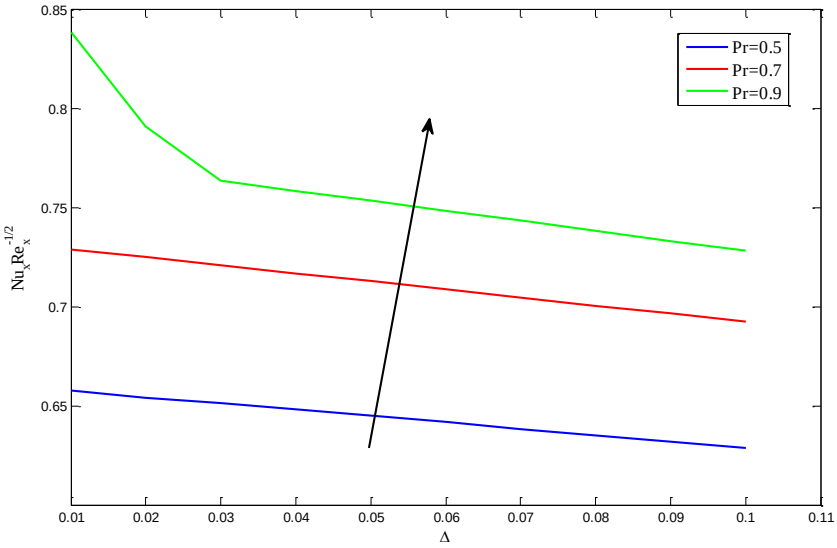

Fig.20 Variation of Nusselt number against Prandtl number

Figure 20 displays the variation of Prandtl number along with the Nusselt number, according to this graph on increasing the value of Prandt number the value of l Nusselt number also raises

II. Conclusions

- Velocity of the fluid increases with the increasing the value of magnetic parameter, coupling parameter, spin gradient viscosity parameter, Jeffery fluid parameter, porosity parameter and micro-inertia density parameter.
- The velocity profile decreases as Deborah number increases but after reaching $\eta = 1.697$ the velocity profile increase.
- Velocity of the fluid decreases while increases the heat generation, Lewis number and Prandtl number.
- The value of micro-rotation increases as spin gradient viscosity parameter increases but after reaching $\eta = 1.364$ the value of micro-rotation decreases.
- The value micro-rotation will decrease until it reaches the $\eta = 1.97$, then it will start to increase certainly.
- Temperature profile increases when the value of heat generation and Prandtl number increases.
- Concentration profile increases, increases the value of Lewis parameter and Prandtl number.
- The skin friction coefficient increases when the value of Deborah number increases.
- On increasing the value of Prandtl number, the value of Nusselt number also increases.

References

[1]. Eringen, A. C. (1966). Theory of micropolar fluids. Journal of Mathematics and Mechanics, 1-18.
[2]. Hayat, T., & Mustafa, M. (2010). Influence of thermal radiation on the unsteady mixed convection flow of a Jeffrey fluid over a stretching sheet. Zeitschrift für Naturforschung A, 65(8-9), 711-719.
[3]. Hayat, T., Shehzad, S. A., Qasim, M., & Obaidat, S. (2012). Radiative flow of Jeffery fluid in a porous medium with power law heat flux and heat source. Nuclear Engineering and Design, 243, 15-19.
[4]. Nadeem, S., Zaheer, S., & Fang, T. (2011). Effects of thermal radiation on the boundary layer flow of a Jeffrey fluid over an exponentially stretching surface. Numerical Algorithms, 57(2), 187-205.
[5]. Turkyilmazoglu, M., & Pop, I. (2013). Exact analytical solutions for the flow and heat transfer near the stagnation point on a stretching/shrinking sheet in a Jeffrey fluid. International Journal of Heat and Mass Transfer, 57(1), 82-88.
[6]. Qasim, M. (2013). Heat and mass transfer in a Jeffrey fluid over a stretching sheet with heat source/sink. Alexandria Engineering Journal, 52(4), 571-575.
[7]. Sharma, B. D., Yadav, P. K., & Filippov, A. (2017). A Jeffrey-fluid model of blood flow in tubes with stenosis. Colloid Journal, 79(6), 849-856.
[8]. Nallapu, S., & Radhakrishnamacharya, G. (2014). Jeffrey fluid flow through porous medium in the presence of magnetic field in narrow tubes. International Journal of Engineering Mathematics, 2014.
[9]. Agarwal, V., Singh, B., & Nisar, K. S. (2022). Numerical analysis of heat transfer in magnetohydrodynamic micropolar jeffery fluid flow through porous medium over a stretching sheet with thermal radiation. Journal of Thermal Analysis and Calorimetry, 1-23.
[10]. Ellahi, R., Rahman, S. U., & Nadeem, S. (2014). Blood flow of Jeffrey fluid in a catherized tapered artery with the suspension of nanoparticles. Physics Letters A, 378(40), 2973-2980.
[11]. Khan, A., Zaman, G., & Algahtani, O. (2018). Unsteady Magnetohydrodynamic Flow of Jeffrey Fluid through a Porous Oscillating Rectangular Duct. Porosity Process. Technol. Appl, 125-128.

[12]. Vaidya, H., Rajashekhar, C., Divya, B. B., Manjunatha, G., Prasad, K. V., & Animasaun, I. L. (2020). Influence of transport properties on the peristaltic MHD Jeffrey fluid flow through a porous asymmetric tapered channel. Results in Physics, 18, 103295.
[13]. Das, K., Acharya, N., & Kundu, P. K. (2015). Radiative flow of MHD Jeffrey fluid past a stretching sheet with surface slip and melting heat transfer. Alexandria Engineering Journal, 54(4), 815-821.
[14]. Agarwal, V., Singh, B., Kumari, A., Jamshed, W., Nisar, K. S., Almaliki, A. H., & Zahran, H. Y. (2021). Steady Magnetohydrodynamic Micropolar Fluid Flow and Heat and Mass Transfer in Permeable Channel with Thermal Radiation. Coatings, 12(1), 11.
[15]. Reddy, Y. D., Goud, B. S., Nisar, K. S., Alshahrani, B., Mahmoud, M., & Park, C. (2023). Heat absorption/generation effect on MHD heat transfer fluid flow along a stretching cylinder with a porous medium. Alexandria Engineering Journal, 64, 659-666.
[16]. Mahabaleshwar, U. S., Sneha, K. N., Chan, A., & Zeidan, D. (2022). An effect of MHD fluid flow heat transfer using CNTs with thermal radiation and heat source/sink across a stretching/shrinking sheet. International Communications in Heat and Mass Transfer, 135, 106080.
[17]. Pandey, A. K., Bhattacharyya, K., Gautam, A. K., Rajput, S., Mandal, M., Chamkha, A. J., & Yadav, D. (2022). Insight into the relationship between non-linear mixed convection and thermal radiation: the case of Newtonian fluid flow due to non-linear stretching. Propulsion and Power Research.
[18]. Megahed, A. M., Reddy, M. G., & Abbas, W. (2021). Modeling of MHD fluid flow over an unsteady stretching sheet with thermal radiation, variable fluid properties and heat flux. Mathematics and Computers in Simulation, 185, 583-593.
[19]. Krishna, M. V. (2020). Hall and ion slip impacts on unsteady MHD free convective rotating flow of Jeffreys fluid with ramped wall temperature. International Communications in Heat and Mass Transfer, 119, 104927.
[20]. Khader, M. M., & Sharma, R. P. (2021). Evaluating the unsteady MHD micropolar fluid flow past stretching/shirking sheet with heat source and thermal radiation: Implementing fourth order predictor–corrector FDM. Mathematics and Computers in Simulation, 181, 333-350.
[21]. Pop, I., & Na, T. Y. (1998). A note on MHD flow over a stretching permeable surface. Mechanics Research Communications, 25(3), 263-269.
[22]. Mbeledogu, I. U., Amakiri, A. R. C., & Ogulu, A. (2007). Unsteady MHD free convective flow of a compressible fluid past a moving vertical plate in the presence of radiative heat transfer. International journal of heat and mass transfer, 50(9-10), 1668-1674.
[23]. Muthucumaraswamy, R., & Sivakumar, P. (2016). MHD flow past a parabolic flow past an infinite isothermal vertical plate in the presence of thermal radiation and chemical reaction. International Journal of Applied Mechanics and Engineering, 21(1).
[24]. Raju, R. S., Reddy, G. J., Rao, J. A., Rashidi, M. M., & Gorla, R. S. R. (2016). RETRACTED: Analytical and numerical study of unsteady MHD free convection flow over an exponentially moving vertical plate with Heat Absorption.
[25]. Adegbie, S. K., Koṛikọ, O. K., & Animasaun, I. L. (2016). Melting heat transfer effects on stagnation point flow of micropolar fluid with variable dynamic viscosity and thermal conductivity at constant vortex viscosity. Journal of the Nigerian Mathematical Society, 35(1), 34-47.
[26]. Malik, M. Y., Bibi, M., Khan, F., & Salahuddin, T. (2016). Numerical solution of Williamson fluid flow past a stretching cylinder and heat transfer with variable thermal conductivity and heat generation/absorption. AIP Advances, 6(3), 035101.
[27]. Misra, J. C., Sinha, A., & Shit, G. C. (2011). Mathematical modeling of blood flow in a porous vessel having double stenoses in the presence of an external magnetic field. International Journal of Biomathematics, 4(02), 207-225.
[28]. Eldabe, N., Agoor, B. M., & Alame, H. (2014). Peristaltic motion of non-Newtonian fluid with heat and mass transfer through a porous medium in channel under uniform magnetic field. Journal of Fluids, 2014.
[29]. Cheng, J., Liao, S., & Pop, I. (2005). Analytic series solution for unsteady mixed convection boundary layer flow near the stagnation point on a vertical surface in a porous medium. Transport in porous media, 61(3), 365-379.
[30]. Ahmed, M. A. M., Mohammed, M. E., & Khidir, A. A. (2015). On linearization method to MHD boundary layer convective heat transfer with low pressure gradient. Propulsion and Power Research, 4(2), 105-113.
[31]. Butt, A. R., Abdullah, M., Raza, N., & Imran, M. A. (2017). Influence of non-integer order parameter and Hartmann number on the heat and mass transfer flow of a Jeffery fluid over an oscillating vertical plate via Caputo-Fabrizio time fractional derivatives. The European Physical Journal Plus, 132(10),